Development of a microfurnace dedicated to in situ scanning electron microscope observation up to 1300 °C. II. Study of the thermal response of samples

Jérôme Mendonça, Henri-Pierre Brau, Dorian Nogues, Antoine Candeias, Renaud Podor

Development of a microfurnace dedicated to *in situ* Scanning Electron Microscope observation up to 1300°C - Part II: Study of the thermal response of samples.

Jérôme MENDONÇA [1,2], Henri-Pierre BRAU [1], Dorian NOGUES [2],
Antoine CANDEIAS [2], Renaud PODOR [1*]

[1] ICSM, Univ Montpellier, CNRS, CEA, ENSCM, Bagnols-sur-Cèze, France
[2] NewTec Scientific, 2 route de Sommières, 30820 CAVEIRAC

* Corresponding author

e-mail: renaud.podor@cea.fr

Tel: 00 (33) 04.66.33.92.02

Mailing addresses:

Dr Jérôme MENDONÇA

NewTec Scientific

2 route de Sommières

30820 CAVEIRAC

FRANCE

Henri-Pierre BRAU

Institut de Chimie Séparative de Marcoule

Site de Marcoule, Bâtiment 426

BP 17171

F-30207 Bagnols sur Cèze Cedex

France

Dorian NOGUES

NewTec Scientific

2 route de Sommières

30820 CAVEIRAC

FRANCE

Antoine CANDEIAS

NewTec Scientific

2 route de Sommières

30820 CAVEIRAC

FRANCE

Renaud PODOR

Institut de Chimie Séparative de Marcoule

Site de Marcoule, Bâtiment 426

BP 17171

F-30207 Bagnols sur Cèze Cedex

France

Abstract: When conducting *in situ* experiments at high temperatures in a SEM using microfurnaces, controlling the temperature of a sample of a few mm^3 placed on the hot zone of the furnace can be a complex task. In most cases, the temperature of the sample is estimated by means of a thermocouple placed in the hot body of the furnace, and the assumption made is that the temperature of the furnace is the temperature of the sample. In this work, a detailed understanding of the thermal response of the sample placed on the hot zone of the furnace is proposed. Temperature differences due to contact resistance between the furnace surface and the sample, the nature of the sample and the sample geometry are calculated with a numerical model and measured experimentally on a dedicated test bench. Three technical solutions (bonding, sandwiching, mini-crucible) for limiting temperature differences between furnace surface and sample are proposed and validated by numerical calculations and experimental measurements.

1. Introduction

This article is the second part of a work dedicated to the development and characterization of a FurnaSEM microfurnace, designed and manufactured to perform high-temperature *in situ* experiments in the chamber of a scanning electron microscope (SEM). In the first part of this work, the thermal behavior of the microfurnace was characterized without taking into account the interaction between the furnace and the sample placed on the hot zone.

Understanding the heat transfer between the furnace and a sample is essential for controlling the sample temperature under actual *in situ* experimental conditions in the SEM chamber. Usually, due to the limited size of the sample (a μm^3 to a few mm^3), it is not possible to place a temperature sensor (such as a thermocouple) directly on the sample [1]. Also, for practical reasons, the heating devices generally used to carry out these studies do not allow the temperature of the sample to be measured directly. For this, the thermocouple must be in direct contact with the sample for accurate temperature measurement [2]. This is usually achieved by welding or bonding the temperature sensor to the sample surface. This is most of the time not possible here, given the small dimensions of the samples. A simple way to determine the temperature of a sample is to measure its melting point. Furnace temperatures are sometimes calibrated by measuring the melting points of pure metals. Temperatures are then linearly interpolated from this value and the ambient temperature [3,4,5]. However, this technique can be difficult to implement, and furnace calibration should be reviewed when operating conditions (gas pressure in the chamber, nature of the gas used) change.

Other technological solutions have been implemented in various studies. A thermocouple has been welded to a metal sample [6,7,8], but this leads to significant local thermal

disturbances and potential chemical reactivity between the thermocouple and the sample. Infrared pyrometry can also be used for non-contact *in situ* sample temperature measurements [9]. This technique requires a good knowledge of the emissivity of the sample (which is a function of its chemical composition, but also of its surface condition) and the ability to position an optical fiber that allows direct reading of the sample temperature. These two constraints are difficult to meet, since the surface composition of samples can change during the course of an experiment (e.g. through oxidation), as can their roughness (formation of oxides, dewetting, etc.). This solution is interesting in special cases, but not universal. Another solution that has been implemented is to integrate the thermocouple head directly into the hot zone of the furnace and place the sample directly on top [4,10,11]. All these technical solutions cannot be implemented on a general basis, therefore temperature measurement is generally carried out on the furnace itself, by positioning a thermocouple close to the hot zone of the furnace [12,13,14,15,16]. The sample temperature is then deduced on the assumption that the heating device is sufficiently efficient for the furnace and sample temperatures to be identical. This assumption is based on specific experimental conditions that are not systematically verified [9].

The aim of this study is to understand how a sample placed on the hot zone of the FurnaSEM microfurnace is heated, using a numerical approach that will then be supported by experimental measurements. The overall results should make it possible to draw up recommendations for using the FurnaSEM microfurnace in high-temperature experiments, and more generally to provide scientists with explanations and answers to problems often encountered and dealt with empirically [17], using a dual numerical and experimental approach.

2. Material and methods

The methods used in this work are those described in the first part of this work [18]. The main points related to these techniques are summarized below.

2.1. Software for modeling heat transfer

To determine the thermal characteristics of a sample deposited on the hot zone of the FurnaSEM microfurnace, numerical simulations of heat transfer are carried out using Flow Simulation©, a commercial software package integrated into the SolidWorks© software suite (Dassault system). This software simulates the 3 modes of heat transfer (conduction, convection and radiation) by numerical discretization using the finite volume method. Calculations will be based on the numerical furnace model developed by Mendonça *et al* [18].

2.2. Test bench

A special test bench has been developed to measure the temperature of the microfurnace and produce heat maps of the microfurnace surface. The test bench is a home-made equipment that can be placed under low or high vacuum (10^{-3} – 300 Pa), simulating the interior of a SEM chamber. It is equipped with an PI1M thermal camera (OPTRIS GmbH) for furnace surface thermography. This instrument uses a CMOS detector capable of recording 382 × 288 pixels sized thermal images at a framerate of 27 Hz. According to the manufacturer, the temperature resolution (i.e. the noise equivalent temperature difference – NETD) of the sensor is 1 K for objects below 700°C and 2 K for objects below 1000°C (for objects at 1400°C it is assumed to be lesser than 2.5 K). Given the camera working distance in the test bench, the spatial resolution (i.e. instantaneous field of view – IFOV) is equals to 0.22 µm/pixel. The raw thermal maps recorded are then digitally processed to take account of the emissivity parameters of the various materials, and of the sample in particular. A substantial change in the test bench compared to the previous work is the integration of a gas control valve (model EVR 116 from Pfeiffer Vacuum) which was used to increase the enclosure pressure up to 1500 – 1600 Pa. This tool was specifically used for a test carried out with a platinum sample placed between the furnace and a thin platinum disc.

2.3. Materials

Reference samples were selected to conduct this study:

- 300 µm-thick platinum laminate foils (Goodfellow)
- 100 µm-thick diamond-polished alumina (Al_2O_3) wafers (Goodfellow)
- Gold filaments 275 µm in diameter (Goodfellow)

These samples were selected for the following reasons: the platinum foils are made of the same material as the hot zone of the FurnaSEM microfurnace, thus color contrast in thermal maps will directly reflect temperature drift. Gold filaments were chosen because their melting point of 1064°C can easily be reached with the microfurnace. Al_2O_3 wafers are used as an inert interface for samples potentially reactive with - or likely to degrade - the hot zone of the furnace. In this case, it is important to ensure that these wafers can transfer heat to a sample placed on them without generating a temperature gradient.

3. Modeling the furnace-sample heat transfer

3.1. 2D steady-state conduction model

First, the study is carried out by modeling the heat transfers taking place within a sample. The aim is to determine the spatial temperature distribution during an isothermal plateau. For the sake of simplicity, two simple geometries - plate and cylinder - of a homogeneous, solid sample are considered. Sample heating is assumed to be homogeneous, and is performed in high vacuum mode to neglect convection. Only radiative heat loss is considered. In summary, the thermal problem corresponds to heating the sample at a temperature imposed on the underside of the sample, simulating the situation where it is placed on the hot zone of the microfurnace. At thermal equilibrium, a 2D temperature profile is calculated on the characteristic half-plane of the geometry being considered (axial symmetry). The two configurations studied and the mathematical models associated with the thermal problem are shown in **Figure 1**.

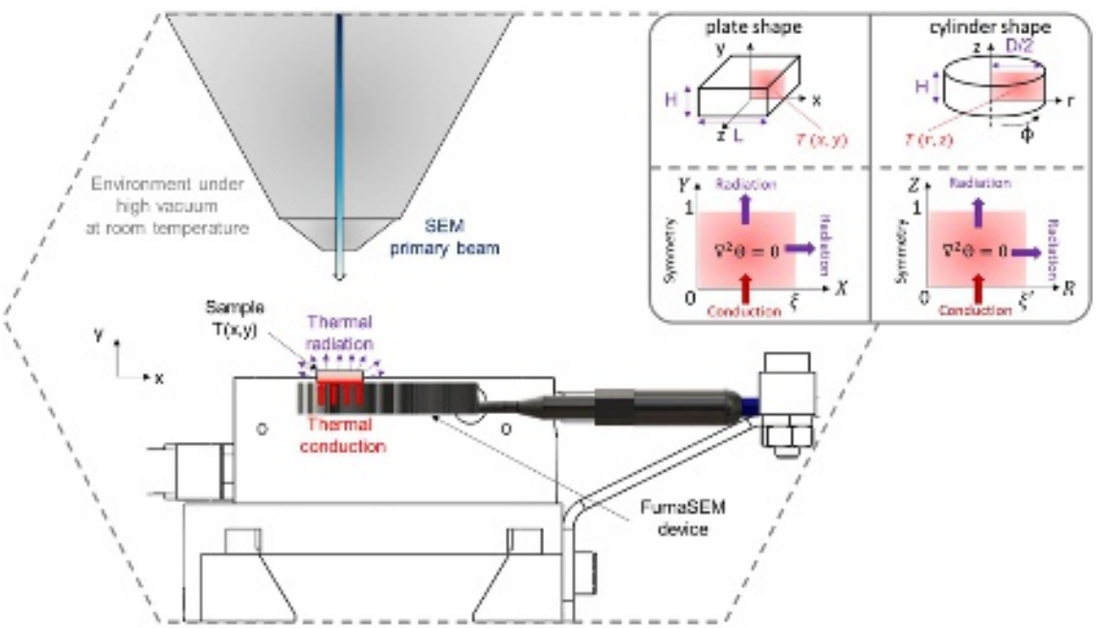

Figure 1 - Diagram of the situation studied where a single sample is heat-treated with FurnaSEM microfurnace in high vacuum mode. The sample is assimilated to a plate or cylinder and radiates freely into the SEM chamber. Geometries and thermal problems are exposed in the top-right insert.

To make the results independent of the absolute dimensions of the sample, the steady-state heat equation is normalized by performing the following variable changes:

$$\begin{cases} \Theta = \dfrac{T - T_\infty}{T_c - T_\infty}\ (adimensional\ temperature) \\ X = \dfrac{x}{H}\ (adimensional\ length\ -\ plate) \\ Y = \dfrac{y}{H}\ (adimensional\ thickness\ -\ plate) \\ \xi = \dfrac{L}{2H}\ (aspect\ ratio\ -\ plate) \\ R = \dfrac{r}{H}\ (adimensional\ radius\ -\ cylinder) \\ Z = \dfrac{z}{H}\ (adimensional\ thickness\ -\ cylinder) \\ \xi' = \dfrac{D}{2H}\ (aspect\ ratio\ -\ cylinder) \end{cases} \quad (1)$$

Where T_c corresponds to the imposed heating temperature and T_∞ to the ambient temperature in the chamber. The "aspect ratio" parameters ξ and ξ' are defined for the two geometries considered, plate and cylinder. They reflect the flatness or height of a sample. From the system (1), the normalized heat equation is defined as:

$$\begin{cases} \dfrac{\partial^2\Theta}{\partial X^2} + \dfrac{\partial^2\Theta}{\partial Y^2} = 0\ (plate) \\ \dfrac{1}{R}\dfrac{\partial\Theta}{\partial R} + \dfrac{\partial^2\Theta}{\partial R^2} + \dfrac{\partial^2\Theta}{\partial Z^2} = 0\ (cylinder) \end{cases} \quad (2)$$

The boundary conditions consistent with the problem are:

- <u>For the plate:</u>

$$\begin{cases} \Theta\ (\mathrm{X}, 0) = 1\ (furnace\ heating) \\ \left.\dfrac{\partial\Theta}{\partial X}\right|_{X=0} = 0\ (axial\ symmetry) \\ \left.\dfrac{\partial\Theta}{\partial X}\right|_{X=\xi} = -\,B_i \times \Theta\ (lateral\ radiative\ losses) \\ \left.\dfrac{\partial\Theta}{\partial Y}\right|_{Y=1} = -\,B_i \times \Theta\ (radiative\ losses\ top\ side) \end{cases} \quad (3)$$

- <u>For the cylinder:</u>

$$\begin{cases} \Theta(\mathrm{R}, 0) = 1\ (furnace\ heating) \\ \left.\dfrac{\partial\Theta}{\partial R}\right|_{R=0} = 0\ (axial\ symmetry) \\ \left.\dfrac{\partial\Theta}{\partial R}\right|_{R=\xi'} = -\,B_i \times \Theta\ (lateral\ radiative\ losses) \\ \left.\dfrac{\partial\Theta}{\partial Z}\right|_{Z=1} = -\,B_i \times \Theta\ (radiative\ losses\ top\ side) \end{cases} \quad (4)$$

Boundary conditions (3) and (4) give rise to a dimensionless number, Bi, known as the Biot number. In our problem, it is defined by:

$$B_i = \frac{h_r \times H}{k} = \frac{\varepsilon \times \sigma \times (T^2 + T_\infty^2) \times (T + T_\infty) \times H}{k} \quad (5)$$

Where h_r is a radiative exchange coefficient defined on the basis of Stefan-Boltzmann's law, such that:

$$\varepsilon \times \sigma \times (T^4 - T_\infty^4) \equiv h_r \times (T - T_\infty) \quad (6)$$

σ is the Stefan-Boltzmann constant, H is the sample thickness and k is its thermal conductivity. Equations (2) with boundary conditions (3) and (4) can be solved using the separation of variables method. This method yields solutions in the form of integer series expansions of hyperbolic functions. The details about the mathematical solving procedure are available in supplementary information **SI**. A general solution of the problem can be formulated as:

$$\Theta(\tilde{X}, \tilde{Y}) = C_{geometry} \times \sum_{n=1}^{\infty} [A_n \cosh(\Lambda_n G_{geometry}) + B_n \sinh(\Lambda_n \tilde{Y})] \times f_n(\tilde{X}) \quad (7)$$

Where $\tilde{X}\ et\ \tilde{Y}$ are the type of dimensionless coordinates considered (cartesian for the plate and cylindrical for the cylinder), $C_{geometry}$ and $G_{geometry}$ are parameters that depends on the geometry, A_n and B_n are coefficients of the series, Λ_n are the eigenvalues of the problem and $f_n(\tilde{X})$ the eigenvectors. **Table 1** summarizes the expression of these various terms for the plate and cylinder.

Table 1 - Analytical expressions for general solution parameters for plate and cylinder geometries

	Plate	**Cylinder**
Coordinate system	X, Y	R, Z
$C_{geometry}$	1	$\left(1 - \frac{Bi}{Bi+1} Z\right)$
$G_{geometry}$	X	$(1 - Z)$
A_n	$A_n = \frac{2(-1)^n Bi \sqrt{(\Lambda_n^2 + Bi^2)}}{\Lambda_n [\xi \Lambda_n^2 + Bi(\xi Bi + 1)]}$	$A_n = \frac{2Bi}{\xi' \cosh(\Lambda_n) J_0(\Lambda_n \xi') (\Lambda_n^2 + Bi^2)}$
B_n	$B_n = -A_n \frac{\Lambda_n \sinh(\Lambda_n) + Bi \cosh(\Lambda_n)}{\Lambda_n \cosh(\Lambda_n) + Bi \sinh(\Lambda_n)}$	$B_n = 0$
$f_n(\tilde{X})$	$f_n(X) = \cos(\Lambda_n X)$	$f_n(R) = J_0(\Lambda_n R)$
Λ_n	$\Lambda_n \sin(\Lambda_n \xi) = Bi \cos(\Lambda_n \xi)$	$\Lambda_n J_1(\Lambda_n \xi') = Bi\, J_0(\Lambda_n \xi')$

From these expressions, normalized temperature profiles can be constructed as a function of the parameters Bi et ξ. The thermophysical properties and dimensions of the specimen are

implicitly embedded in these parameters thus it will condition the thermal profile obtained. On **Figure 2** and **Figure 3** are displayed normalized 2D heat maps calculated as a function of the values considered for the plate and cylinder. The penetration of the hot temperature $\Theta = 1$ into the solid depends directly on the values of Bi and ξ. The most uniform profiles are obtained with values $\xi = 10$ and $Bi = 0.1$ corresponding to thin samples with high thermal conductivity. According to equation (5), the Biot number depends on material properties and working temperature. In experimental conditions where it is difficult to have $Bi \leq 0.1$, the aspect ratio ξ can be increased to very large values to limit temperature gradients. In practice, this means reducing the thickness of the sample for the same surface area.

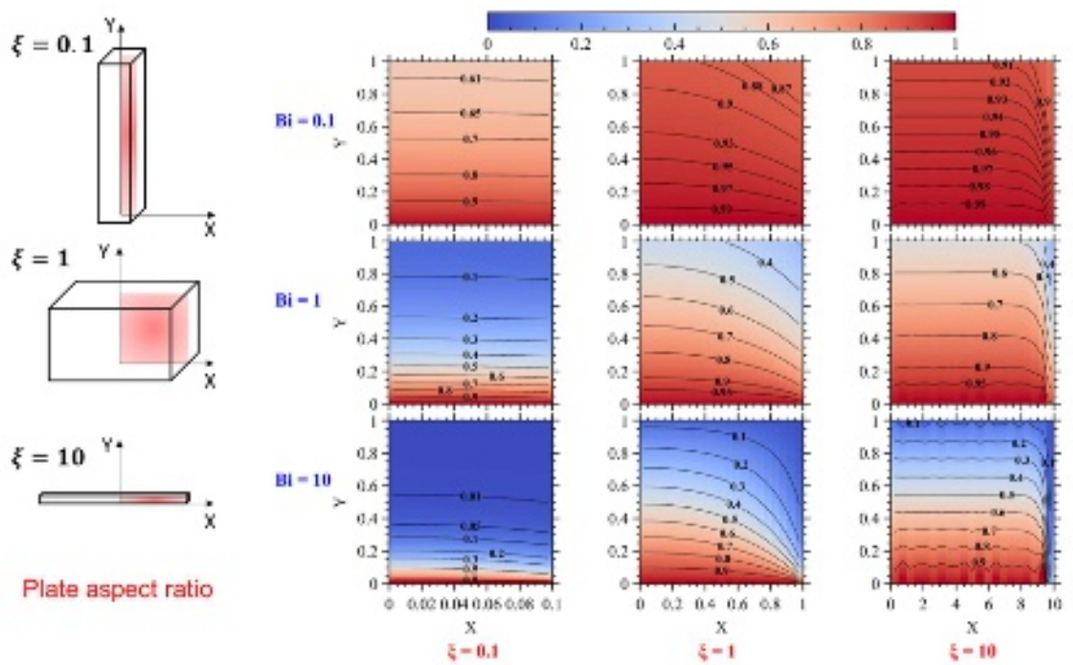

Figure 2 - Normalized plate temperature profiles as a function of Bi number and aspect ratio ξ.

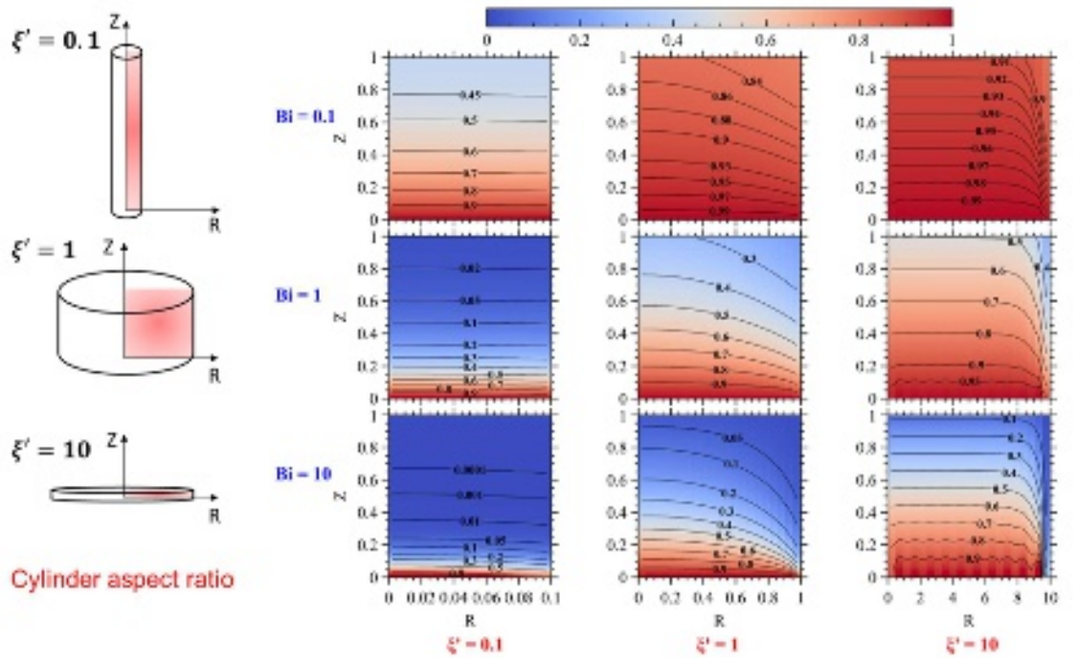

Figure 3 - Normalized cylinder temperature profiles as a function of Bi number and aspect ratio ξ'.

The normalized profiles plotted are not easy to interpret directly. Therefore, they are used to construct explicit heat maps of a finite sample size, as a function of its chemical composition and heating conditions. 4 examples of temperature profiles have been calculated for a cylinder of 2 mm radius and 1 mm height, made from 4 different materials and heated to 1300°C. The profiles are shown in **Figure 4** and the main results are summarized in **Table 2**. In agreement with the interpretations derived from the standardized thermal maps, the magnitude of temperature heterogeneities is directly related to the value of the sample's Bi number. Insulating and highly emissive materials are particularly difficult to heat homogeneously to 1300°C. This is the case with alumina cylinders, where the surface not directly exposed to the heat flow shows temperature differences of up to 50°C in some areas of the sample, compared to the temperature of the hot substrate. To limit these thermal gradients, it is recommended that samples be thinned as much as possible until they have $Bi \leq 10^{-3}$. Samples meeting this criterion are referred to as "thermally thin" and can be considered to have a uniform temperature throughout their volume. These data demonstrate that the behavior of metallic samples with good thermal conductivity can be studied in high-temperature SEM on relatively massive (i.e. thick) samples.

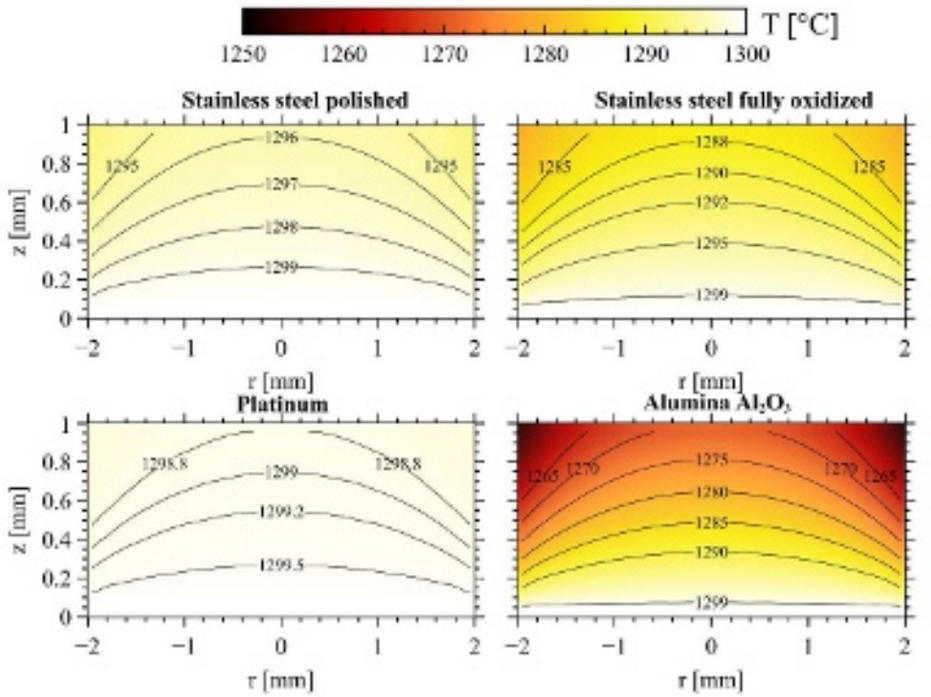

Figure 4 - Explicit temperature profiles calculated for cylindrical samples, radius 2 mm, height 1 mm, of different chemical compositions, heated to 1300°C.

Table 2 - Material properties and main data obtained from thermal profiles established at 1300°C for a cylindrical geometry with a radius of 2 mm and a height of 1 mm

	Stainless steel polished	**Stainless steel fully oxidized**	**Platinum**	**Alumina**
k [W/m.K] (at 1300°C)	30.70	30.70	87.42	5.97
emissivity ε	0.32	0.97	0.20	0.45
Bi number ($\times 10^{-3}$)	2.774	8.434	0.621	19.630
Max T [°C]	1300.00	1300.00	1300.00	1300.00
Min T [°C]	1293.34	1279.74	1298.23	1253.29
Mean T [°C]	1297.41	1292.02	1299.17	1281.41
Standard deviation [°C]	**1.67**	**5.05**	**0.42**	**11.64**

3.2. Real heating at the furnace-sample interface

In a real-life situation where the sample is simply placed on the hot zone of the furnace, the sample temperature may remain below the furnace surface temperature, even if every effort is made to ensure that the thermally thin body condition is verified. Indeed, the simple 2D conduction model developed previously does not take into account the efficiency of

interfacial heat transfer between the surface of the sample holder and the sample. For these numerical simulations, it was implicitly assumed that no surface discontinuity existed between these two elements, and the lower temperature of the sample was always considered equal to the temperature of the hot zone of the furnace. This assumption is generally accepted when carrying out *in situ* experiments at high temperatures in the SEM, as it allows a simple estimation of the sample temperature. In reality, surface roughness and the non-planarity of samples placed on the hot support can reduce heat transfer and limit thermal conduction at the interface of the two elements. A real interface is where there are both solid-solid "spot contacts" and "empty gaps" where no contact exists between the two surfaces [19,20,21]. Schematically, the interface can be considered as a porous heterogeneous region (**Figure 5**). The existence of this discontinuity will generate superficial heat propagation, with constriction of heat flow lines at solid-solid contacts. On a macroscopic scale, this phenomenon results in a temperature drift at the sample level.

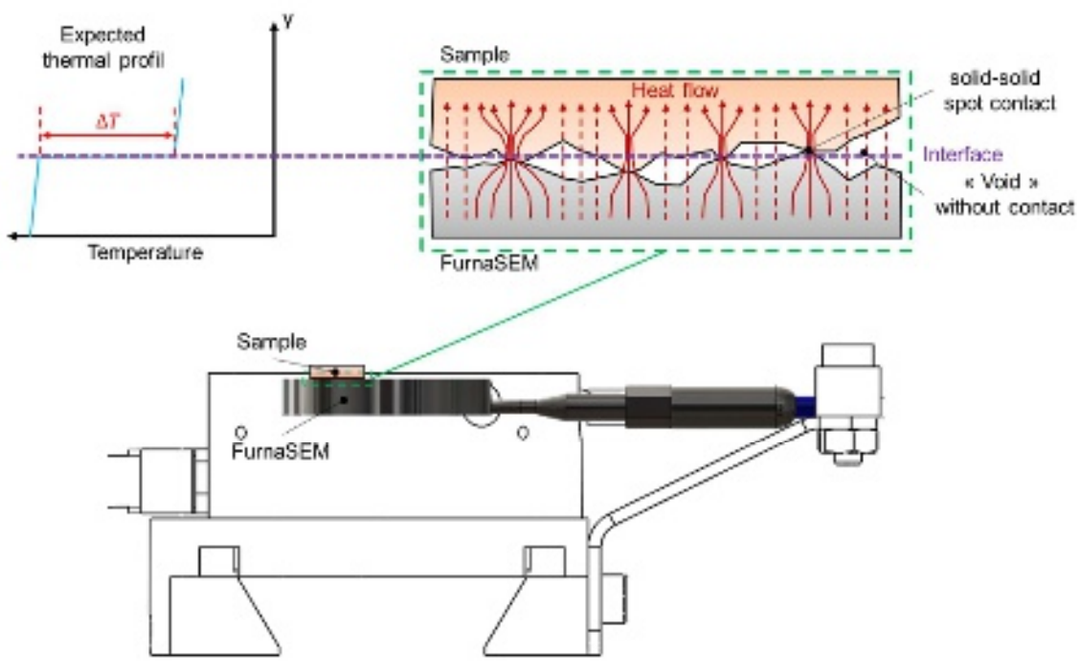

Figure 5 - Schematic representation of a real interface between the sample and the FurnaSEM microfurnace. Surface roughness leads to the appearance of empty spaces called "voids" or "interstices", which limit heat transfer. A temperature discontinuity is expected, as indicated in the top left-hand corner.

Interfacial heat conduction can be modelled using the contact thermal conductance h_c, defined as follows:

$$h_c = \frac{1}{R_{thc}} \equiv \frac{Q}{S_{contact} \times \Delta T_{interface}} \quad (8)$$

Where R_{thc} is the contact thermal resistance, Q the heat flux across the interface, $S_{contact}$ represents the apparent contact area and $\Delta T_{interface}$ is the temperature difference across the interface. The degree of thermal coupling between the FurnaSEM microfurnace hot zone and a sample can be assessed from these parameters. Given a set h_c value, it is possible to model the temperature drift $\Delta T_{interface}$ of the sample under given experimental conditions, assuming nevertheless that it does indeed meet the uniformity criterion ($Bi \leq 10^{-3}$). In the same situation as studied previously (cf. §2.1), the heat balance of the sample can be expressed by:

$$mCp\frac{dT_{sample}}{dt} = h_c \times S_{contact} \times \Delta T_{interface} - \varepsilon \times \sigma \times S_{ray} \times \left(T_{sample}^4 - T_\infty^4\right) \quad (9)$$

Where m is the mass of the sample, Cp its heat capacity, $h_c.S_{contact}.\Delta T_{interface}$ represents the heat flux transmitted by the furnace and $\varepsilon.\sigma.S_{ray}.\left(T_{sample}^4 - T_\infty^4\right)$ is the heat flux lost by radiation in a closed environment assumed to have large dimensions in front of the furnace. At thermal equilibrium, the relationship (9) becomes:

$$\Delta T_{interface} = \frac{\varepsilon \times \sigma \times S_{ray} \times \left(T_{sample}^4 - T_\infty^4\right)}{h_c \times S_{contact}} \quad (10)$$

This relationship makes it possible to quantify the temperature drift likely to occur as a function of heating temperature and interfacial conductance. If we're dealing with a thin sample, S_{ray} can be approximated as the sample area observed with the microscope then we can assume that $S_{ray} = S_{conta}$ and therefore that:

$$\Delta T_{interface} = \frac{\varepsilon \times \sigma \times \left(T_{sample}^4 - T_\infty^4\right)}{h_c} \quad (11)$$

From this expression, we can see that the thermal drift $\Delta T_{interface}$ will be favorized by the occurrence of a poor contact conductance, a high working temperature and a high material emissivity. For a given set of *in situ* experimental conditions (i.e. sample chemical composition and working temperature), the only way to reduce $\Delta T_{interface}$ is by improving the contact conductance. For the purpose of this study, equation (11) will be used to estimate the effective thermal contact conductance of real samples put in the FurnaSEM sample holder throughout the direct measurement of sample temperature (see the next section regarding experimental tests). In the following section, these phenomena will be illustrated by practical examples, and solutions to limit thermal drift will be proposed.

4. Experimental demonstration of temperature drift

To highlight the existence of thermal drift between a sample and the hot zone of the FurnaSEM microfurnace, and to quantify its magnitude, controlled thermal treatments were carried out on the test bench to measure sample temperature using non-contact IR thermography. To overcome the difficulties inherent in temperature measurement by thermography, three reference samples were selected for study (see Materials and methods section for explanations).

Heat treatments were carried out in high vacuum mode, and temperature maps were recorded with the IR camera between 500 and 1300°C. Thermal drift measurements, deduced directly from the sample surface temperature measured with the thermal camera, are plotted in **Figure 6**. The behavior of the samples varies according to their chemical composition. Alumina wafers are the materials tested with the lowest thermal drift. It did not exceed 100°C when the furnace was heated to nearly 1300°C. Platinum foils behave differently, thermal drift is greater, and can reach 200°C to 1300°C (**Figure 6b**). The different heating efficiency between the two material is only due to a difference of thermal contact. The Al_2O_3 wafer is flat and stiff while the Pt foil is softer and slightly bent leading to a few points of direct contact with the hot zone of the furnace. As a result, thermal contact between the platinum foil and the furnace is generally less efficient than that observed with alumina wafers.

In the case of the gold filament, the thermal drift recorded is even greater, given that the filament is deposited on a platinum foil in imperfect contact with the furnace surface. Thermal drift values of up to 250°C, corroborated by the observation of gold wire melting (**Figure 6c**), are measured when the hot zone of the microfurnace is at a temperature of 1300°C. Correlation of these experimental data with theoretical curves calculated using the expression (11) shows that contact conductance h_c is quite variable. Values range from 25 to 50 W/m².K when thermal contacts are poor, to almost 1900 W/m².K in the most favorable case recorded with an alumina wafer.

Moreover, the distribution of experimental points shows that heating does not take place at iso-conductance, as they do not follow the same evolution as the theoretical curves (**Figure 6b** and **Figure 6d**). Indeed, the model only takes into account conductive heat transfer through interfacial conductance. However, as temperature rises, thermal radiation plays a part in heat exchange within interstitial regions. This additional mechanism causes the effective contact conductance to change during heating, but not enough to minimize thermal drift.

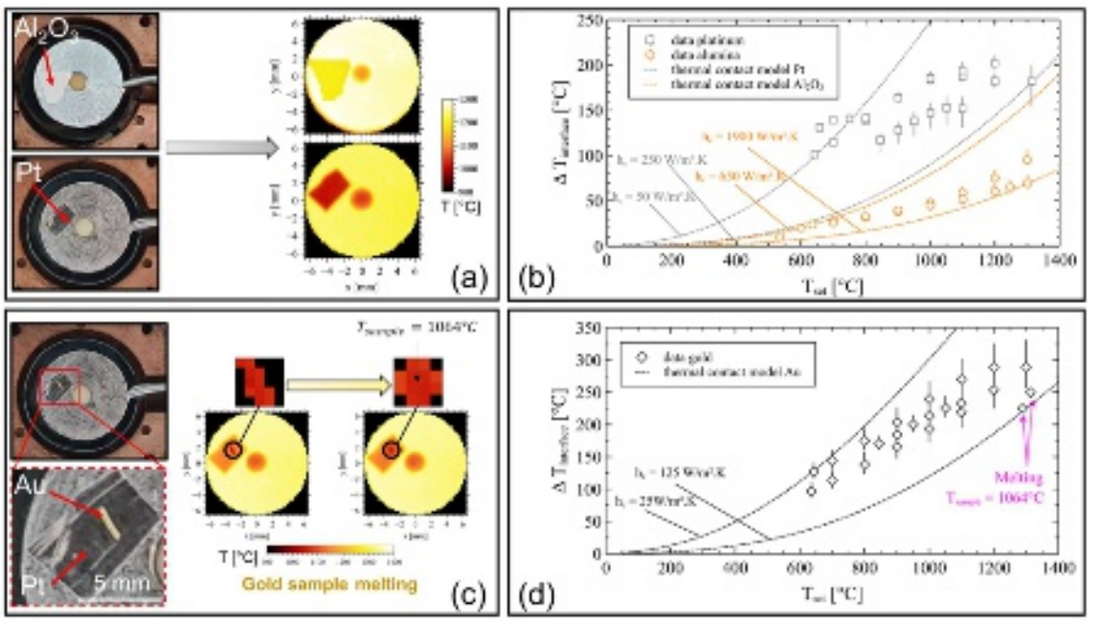

Figure 6 - Measurement of sample temperature and thermal drift by IR thermography. (a) Alumina wafer and platinum foil heat treatments. (b) Evolution of thermal drift associated with the "alumina wafer" and "platinum foil" tests for different steady temperatures set. (c) Heat treatment of a gold wire with observation of melting (reference temperature equal to 1064°C). (d) Evolution of the thermal drift associated with the “gold wire” test for different steady temperatures set.

5. Correction of temperature drift and optimization of contact between the hot zone of the microfurnace and the sample

5.1. Improving heat transfer at interfaces by bonding

Thermal drift measurements carried out on the alumina wafer and platinum foil have shown that the geometry of the sample, particularly its flatness and its surface finish (low roughness), can limit thermal drift at the interfaces. A simple solution for improving interfacial heat transfer (and reducing temperature mismatch between furnace and sample) is to apply an adhesive to bond the sample to the furnace support. However, this adhesive must be chemically inert towards the sample and the microfurnace sample holder, and stable up to 1300°C. A zirconia-based refractory cement (ZrO_2) was used to bond samples to the furnace. Experiments were carried out with this adhesive to verify the suitability of this technical solution for *in situ* experiments. Thermal drift values recorded with a pure platinum sample simply placed on the sample support and bonded to the sample support, then heated under the same conditions up to 1200°C are plotted in **Figure 7**. The use of refractory cement reduces the temperature mismatch between the sample and the hot zone of the furnace. Under these conditions, the residual thermal drift is 30°C for a temperature of 1200°C (compared with 200°C when the

sample is simply laid). Thermal contact conductances calculated from these data range from 1100 to 2370 W/m².K, i.e. 10 times higher than those obtained with the same samples simply laid down.

This technical solution appears to be well suited to limiting thermal mismatch between the sample and the hot zone of the microfurnace. However, this solution may have some drawbacks. Refractory cements are composed of a mineral filler and aqueous and/or organic binders. At high temperatures, they tend to continue to decompose, releasing into the reaction chamber gases that are potentially reactive with the observed surface (oxidation, carburization, etc.). This can lead to real problems when working with high vacuum levels, particularly in the presence of highly reactive materials (such as highly oxidizable metals). In such cases, the advantages of using an all-metal microfurnace like FurnaSEM may be lost. Finally, cleaning the hot zone of the furnace to remove the sample and cement residues can be tricky and lead to a degradation of the furnace's surface finish.

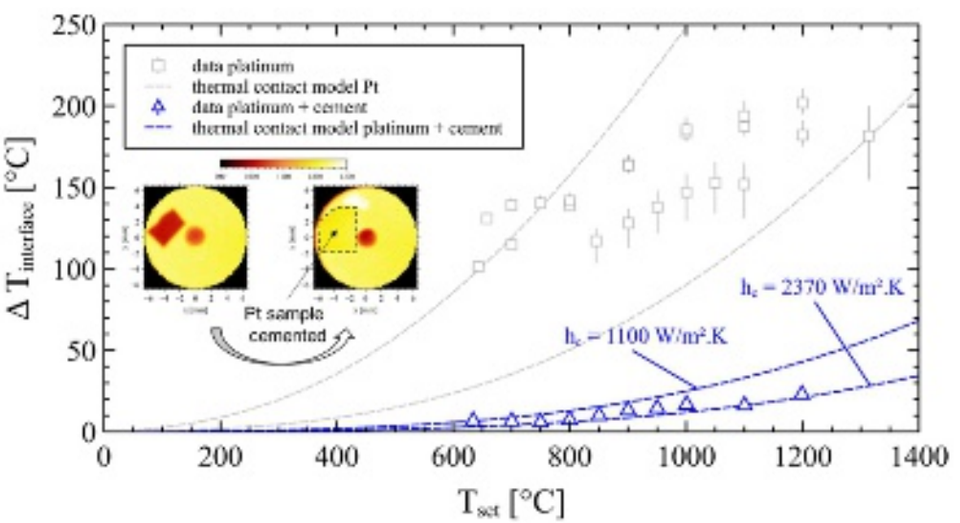

Figure 7 - Comparison of thermal drifts obtained for a platinum sheet simply laid and a sheet bonded with refractory cement. Thermal contact conductance improvement is highlighted by model curves.

5.2. Improving heat transfer at interfaces by sandwiching the sample

Another solution proposed is to sandwich the sample between the hot zone of the furnace and a gold or platinum foil cut to the size of the hot zone of the microfurnace and held upon the hot zone surface. The advantage of this technical solution is that it is easy to install, does not pollute the atmosphere around the sample, does not react with the sample or the hot zone of the furnace (the metal used must be suitable for the temperature range in which the experiments are carried out) and is easy to dismantle (no post-experiment cleaning required).

The sample used is a platinum coupon. This sample is sandwiched between the furnace surface and a gold or platinum disc. The outside diameter of the disc is 13.5 mm (i.e. equal to the furnace diameter) and the disc has a 3 mm hole in its center. The temperature of the sample is measured using the IR thermal camera (sample temperature) and the thermocouple inserted in the hot zone of the furnace (furnace temperature) (**Figure 8**). Most of these tests were carried out under high vacuum. A specific test, carried out at 800°C, was performed under high vacuum and then at different partial vacuum pressures in order to measure the influence of gas pressure on thermal drift response.

When a gold disc is used, the thermal drift recorded is 15°C to 30°C when the furnace temperature is 550 and 950°C respectively (**Figure 8a**). When a platinum disc is used, the thermal drift recorded is more dispersed along tests, which denote a high sensitivity to the mounting quality (**Figure 8b**). In the best case, thermal drift is between 15°C and 55°C for set temperatures of 600 and 1200°C respectively. However, in the worst cases (i.e. when poor contacts are obtained between furnace, disc and sample), thermal drift is between 30°C and 90°C in the same temperature range. Working under vacuum at a pressure of 120 Pa does not significantly alter the results. However, when the pressure in the test bench is increased, a reduction in the magnitude of thermal drift is observed. It is 25°C when the pressure reaches 1500 Pa. This reduction in temperature drift is explained by the presence of a thin layer of hot gas between the furnace and the disc. This layer of gas transports heat from the furnace to the sample, which tends to counterbalance the effect of resistance to thermal conduction. By its very nature, this convective transport is most effective at higher pressures.

Finally, it should be noted that the gold disc can only be used up to 950°C, as interdiffusion between the gold and the hot platinum furnace substrate can cause the disc to weld at higher temperatures. The platinum disc can work at higher temperatures, but unfortunately, the actual disc manufactured and tested induces less efficient heat transfer than the gold disc.

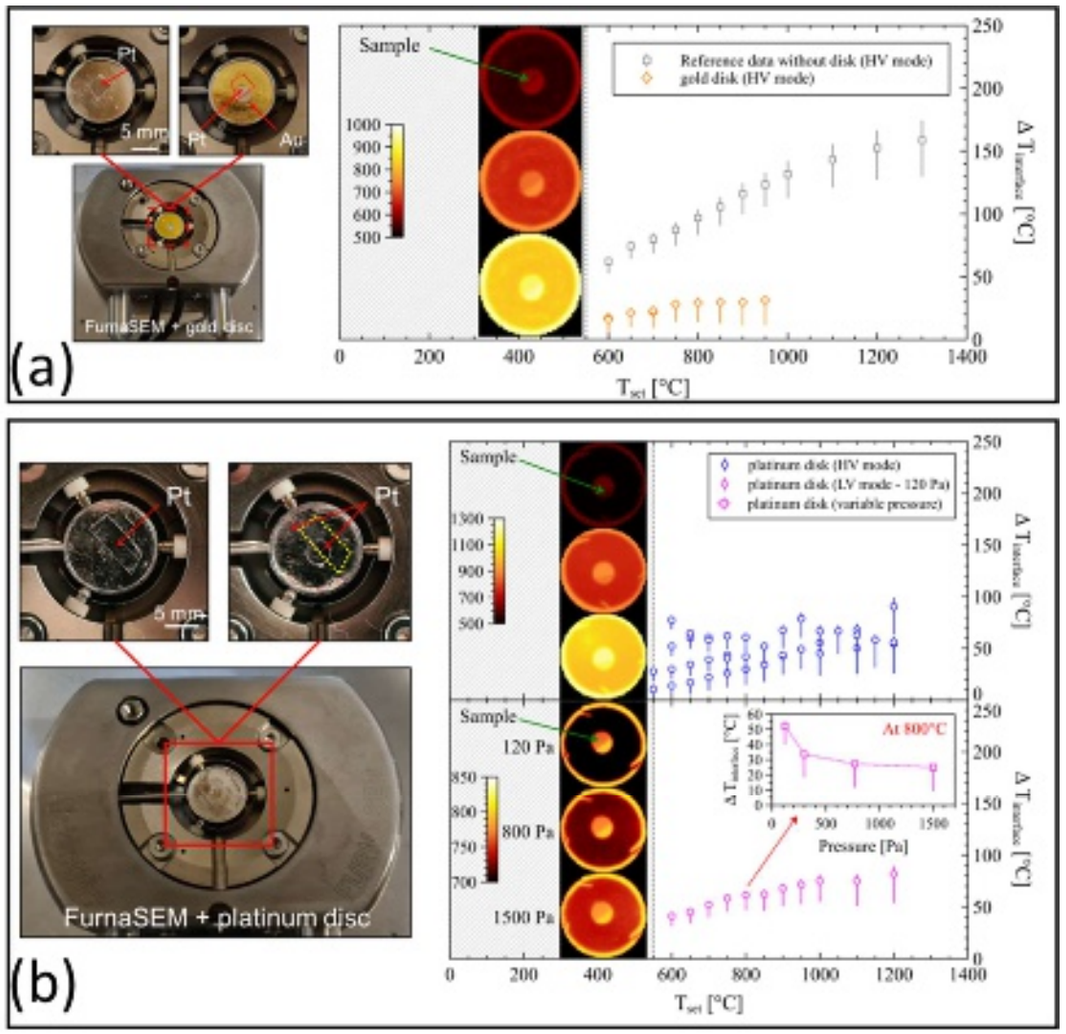

Figure 8 - Experimental tests of the "sandwich" solution carried on an alternate version of FurnaSEM microfurnace. Thermal drift is recorded on a platinum sample with the thermal camera. (a) Photographs of a sample mounted in the microfurnace with the gold disc and corresponding thermal drift data without and with the disc in high vacuum mode. Some thermal maps obtained during tests are shown. (b) Photographs of a sample mounted in the microfurnace with the platinum disc and corresponding thermal drift data acquired with the disc in high vacuum and low vacuum modes. The effect of the atmosphere pressure is measured in the range 120 – 1500 Pa for a set temperature of 800°C.

5.3. Improving heat transfer at interfaces through a “mini-crucible” solution

Some samples do not have the required geometry to be bonded or sandwiched to the furnace surface as described above. This is the case with powder samples. In the case of very fine, dispersible powders, for which the study of isolated grains is necessary, their small size and dispersion on the furnace support ensure that their temperature is equal to the temperature of the hot zone surface. If the powders need to remain aggregated for analysis (e.g. to study

their sintering), one possible solution is to confine them to a small hole drilled in the surface of the hot zone. This hole will form a mini crucible (1 mm in diameter and 1 mm deep, for example) which does not affect the thermal behavior of the FurnaSEM microfurnace, and which can be filled (completely or partially) with the powder to be studied. In this case, the confinement effect and the numerous contacts between the compacted powder and the edges of the mini-crucible limit the temperature difference between the sample and the hot zone. Experimental validation of this solution was not possible due to the technical limitations of the device. Indeed, the thermal camera does not offer sufficient resolution to accurately measure the temperature of a sub-millimeter sample installed in a small hole. Consequently, the evaluation of the mini-crucible solution was based on numerical calculations.

Numerical simulations were carried out to demonstrate the efficiency of the mini crucible when different samples are introduced. To model the mini-crucible, a hole of diameter D and height H was drawn in the virtual microfurnace (**Figure 9a**). Four samples of two different shapes and materials were numerically tested. A 0.5 × 0.5 × 0.3 mm plate of platinum or alumina grain (modeled as a 3 × 3 array of thin cylinders) and a 0.5 mm diameter, 0.3 mm high cylinder of platinum or alumina grain (modeled as a circular array of thin cylinders) were simulated. Poor thermal contact between the sample and the microfurnace is taken into account in the form of a contact thermal conductance h_c of a given value equal to 100 or 1000 W/m².K set at the underside of the sample. The samples are heated with the furnace power set to 40 W, corresponding to a temperature of 1300°C at the thermocouple point. Results obtained are shown in **Figure 9b** to **Figure 9e.**

The results of numerical simulations (carried out for a furnace temperature of 1300°C) show that a significant reduction in thermal drift is obtained as a function of the relative dimensions of the hole. For all samples tested, the thermal drift decreases from 400 - 600°C to a minimum value of 1.5 - 25°C, when moving from a morphology where the sample is placed directly on the furnace surface to a geometry where the sample is placed in a mini-crucible with a depth (H) twice its diameter (D). The value of the height/diameter ratio should be as high as possible to maximize the mini-crucible effect. For a value equal to 2, thermal drift is greatly minimized. A mini-crucible that complies with this geometry (e.g. with a diameter of 500 µm) is relatively easy to install locally on the hot end of the furnace, without degrading furnace capacity. These results show that the "mini-crucible" solution can partially compensate for the imperfect contact observed experimentally. The benefits of this solution can only be demonstrated through numerical simulation.

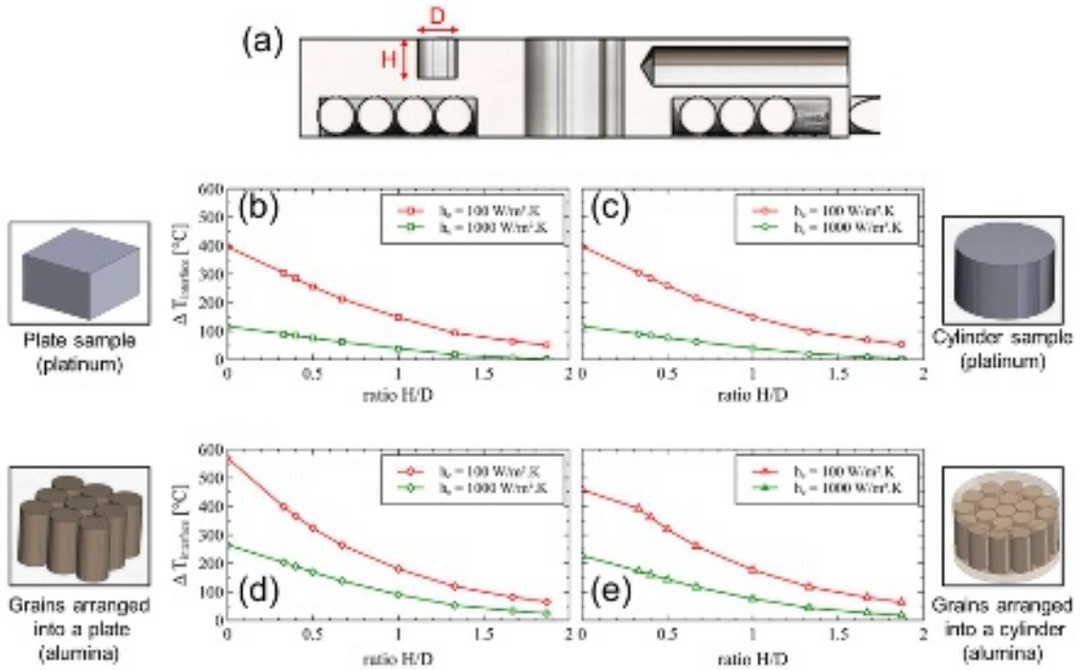

Figure 9 - Sample thermal response simulated for (a) a mini-crucible modelled as a drilled hole in the microfurnace. Simulations were done with a set heat power of 40 W which lead to a 1300°C thermocouple point temperature. The dimensions of the hole are determined by the height/diameter ratio. Thermal drift obtained for (b) a platinum plate, (c) a platinum cylinder, (d) cylindrical alumina grains organized to form a square-based parallelepiped, (e) cylindrical alumina grains organized to form a cylinder. Data reported for two thermal conductance h_c values.

6. Conclusion

In this work, the thermal behavior of a sample placed in the hot zone of the FurnaSEM microfurnace was studied, under conditions representative of those encountered in the chamber of a scanning electron microscope. Two critical points were identified and quantified to optimize the thermal coupling between the FurnaSEM microfurnace hot zone and a sample: the geometry of the sample and its thermal properties, and the thermal contact between the sample and the hot support.

Thanks to a numerical analysis of steady-state 2D conduction, the Biot number was identified as the quantitative criterion to be taken into account to guarantee a homogeneous temperature field over the entire sample volume for the simple geometries considered (plate and cylinder). The mathematical solution of the internal thermal field of a sample heated to high temperature has highlighted the importance of this parameter in distinguishing the behavior of a thermally thin sample (where temperature gradients can be neglected) from that of a thermally thick sample (where temperature gradients are too great to consider the temperature as uniform throughout the sample). To approach the ideal case where the sample

is isothermal over the entire temperature range covered by the FurnaSEM microfurnace, the Biot number must be minimized (i.e. less than or equal to 10^{-3}). To achieve this, the microscopist should ideally use samples with lateral dimensions of between 1 and 4 mm and thicknesses of between 0.1 and 1 mm (for insulating and heat-conducting materials respectively - 1 mm is the maximum value recommended for ease of experimentation).

Standard sample layout on FurnaSEM has shown that the predominant factor impacting thermal coupling is the interfacial thermal resistance induced by a no ideal contact between the hot zone of the microfurnace and the sample. As the contact surfaces are usually rough, heat transfer at the interface between the two solids is limited by the presence of interstices generating a temperature shift during a thermal cycle. This offset depends on the characteristics of the sample and the working temperature, so it cannot be systematically corrected. This phenomenon, experimentally demonstrated by IR thermography, generates temperature jumps of 65 to 250°C over the 600 - 1300°C temperature range.

Three technical solutions have been proposed and implemented to minimize the temperature jump. The sample can be bonded to the surface of the microfurnace using refractory cement. This solution is easy to implement, but not universal. It can lead to the release of gases (which can react with the surface under study) and the cement can be difficult to remove from the furnace surface. Another solution is to sandwich the sample between the hot zone surface and a platinum (or gold) disc. This is a moderate efficient solution, which reduces the temperature jump to 20 - 80°C at 1200°C. Once again, this solution is not universal: it is not suitable for the study of compacted powders, for example. Other solution that is also possible is the excavation of a mini-crucible integrated into the furnace hot zone. This solution has not been validated experimentally for technical reasons, but it has been tested "numerically" using the microfurnace numerical model. This is an interesting solution, as it would reduce the temperature jump, which is minimized to around 1.5 - 25°C at 1300°C for a small and deep hole (heigh to diameter ratio near to a value of 2), and allows working with powders.

The results reported in this work show the particular precautions to be taken when preparing and positioning a sample on the FurnaSEM microfurnace, and more generally in or on miniature furnaces used for experimental equipments (SEM, TEM, XRD, Raman, optical microscopy, etc.). These precautions guarantee the thermal homogeneity of the sample and the representativeness of its temperature measurement with the thermocouple integrated in the microfurnace. More generally, the combination of numerical processing and experimental measurements has enabled us to quantify thermal phenomena that are often observed by users of open miniature furnaces, but dealt with empirically. Here, solutions whose

effectiveness has been quantified have been proposed and implemented. All experimental conditions have been optimized for using the FurnaSEM microfurnace in a SEM chamber, and for carrying out high temperature *in situ* experiments, which are reported in the third part of this work.

SUPPLEMENTARY MATERIALS

Supplementary information: Analytical solutions of 2D heat conduction.

The steady state 2D heat conduction problem is described for a sample taking the form of a plate and a cylinder. General mathematical solutions are obtained by reducing the problem into a dimensionless form. This procedure leads to the introduction of dimensionless parameters “Biot number (Bi)” and “Form factor (ξ)”. The final mathematical expressions for the temperature take the form of an infinite serie expansion of mathematical functions. The computation of the sample temperature field was done by developing the mathematical expressions until the 20^{th} order for a set of Bi and ξ values.

ACKNOWLEDGMENT

The authors would like to thank the following organisations for helping to fund all or part of this work: the Région Occitanie and FEDER (Readynov Project Call) have funded the FurnaSEM project (2018-2021). Jerome Mendonça's PhD thesis (2019-2022) was funded by the Association Nationale de la Recherche et de la Technologie (ANRT) through the Cifre program.

AUTHOR DECLARATIONS

Conflict of Interest

The authors have no conflicts to disclose.

Author Contributions

Jérôme. Mendonça: Writing – original draft (lead); Data curation (lead); Methodology (equal); Investigation (equal).

Henri-Pierre Brau: Data curation (supporting) ; Methodology (equal); Investigation (equal).

Dorian Nogues: Data curation (supporting); Investigation (supporting).

Antoine Candeias: Funding acquisition (equal lead); Conceptualization (Equal).

Renaud. Podor: Funding acquisition (equal lead); Conceptualization (Equal); Data curation (supporting); Investigation (supporting); Writing – review & editing (lead).

DATA AVAILABILITY

The data presented in this manuscript is available from the corresponding author upon reasonable request.

7. References

[1] W. S. Eu, W. H. Cheung, M. Valix, Design and application of a high-temperature microfurnace for an in situ X-ray diffraction study of phase transformation. J. Synchrotron Rad. (2009). 16, 842–848 (doi:10.1107/S090904950903115X)

[2] A. Bank Blichfeld, K. Bakken, D. Chernyshov,b J. Glaum, T. Grande, M.-A. Einarsrud, Experimental setup for high-temperature in situ studies of crystallization of thin films with atmosphere control. J. Synchrotron Rad. (2020) 27 1209-1217(https://doi.org/10.1107/S1600577520010140)

[3] J. M. Cohen, K.J.H. Hartley, M. B. Waldron, A simply constructed heating stage for the scanning electron microscope. J. Microscopy (1980) 118[4] 463-470 (https://doi.org/10.1111/j.1365-2818.1980.tb00296.x)

[4] R. Podor, D. Pailhon, J. Ravaux, H.-P. Brau, Development of an Integrated Thermocouple for the Accurate Sample Temperature Measurement During High Temperature Environmental Scanning Electron Microscopy (HT-ESEM) Experiments. Microsc. Microanal. (2015) 21 307-312 (https://doi.org/10.1017/S1431927615000252)

[5] https://assets.thermofisher.com/TFS-Assets/MSD/Datasheets/high-temperature-stage-esem-datasheet.pdf

[6] J. M. Cohen, K. J. H. Hartley, M. B. Waldron, A simply constructed heating stage for the scanning electron microscope. J. Microscopy (1980) 118[4] 463-470 (https://doi.org/10.1111/j.1365-2818.1980.tb00296.x)

[7] N. Bozzolo, S. Jacomet, R.E. Logé, Fast in-situ annealing stage coupled with EBSD: A suitable tool to observe quick recrystallization mechanisms. Mater. Charac. (2012) 70 28-32 (https://doi.org/10.1016/j.matchar.2012.04.020)

[8] M. Munz, M. T. Langridge, K. K. Devarepally, D. C. Cox, P. Patel, N. A. Martin, G. Vargha, V. Stolojan, S. White, R. J. Curry, Facile Synthesis of Titania Nanowires via a Hot Filament Method

and Conductometric Measurement of Their Response to Hydrogen Sulfide Gas. ACS Appl. Mater. Interfaces (2013) 5 1197−1205 (https://doi.org/10.1021/am302655j)

[9] A. Dimanov, A. El Sabbagh, J. Raphanel, M. Bornert, L. Thiên-Nga, S. Hallais, A. Tanguy, Deformation of aluminum in situ SEM and full field measurements by digital image correlation: evidence of concomitant crystal slip and grain boundary sliding. Materials Science and Engineering A (2022) (http://dx.doi.org/10.2139/ssrn.3922862)

[10] D. M. Kirch, A. Ziemons, T. Burlet, I. Lischewski, X. Molodova, D. A. Molodov, G. Gottstein, Laser powered heating stage in a scanning electron microscope for microstructural investigations at elevated temperatures. Rev. Sci. Instrum. (2008) 79 043902 (https://doi.org/10.1063/1.2908434)

[11] S. K. Verma, G. M. Raynaud, R. A. Rapp, Hot-Stage Scanning Electron Microscope for High-Temperature In-Situ Oxidation Studies. Ox. Metals (1981) 15[5/6] 471-483

[12] R. W. Knowles, T. A. Hardt, High temperature specimen stage and detector for an environmental scanning electron microscope. Patent n° 96928086.6/0 788 653 (08/08/1996) (https://data.epo.org/publication-server/document?iDocId=2751475&iFormat=0)

[13] M. M. Rebbeck, I. Sikorski, A simple inexpensive heated specimen stage for the scanning electron microscope. J. Phys. E: Sci. Instrum. (1988) 21 1106-1107 (https://doi.org/10.1088/0022-3735/21/11/023

[14] R. Heard, J. E. Huber, C. Siviour, G. Edwards, E. Williamson-Brown, An investigation into experimental in situ scanning electron microscope (SEM) imaging at high temperature. Rev. Sci. Instrum. (2020) 91 063702 (doi:10.1063/1.5144981)

[15] L. A. Lumper, G. J.K. Schaffar, M. Sommerauer, V. Maier-Kiener, In-situ microscopy methods for imaging high-temperature microstructural processes – Exploring the differences and gaining new potentials. Materials Science & Engineering (2023) A 887 145738 (https://doi.org/10.1016/j.msea.2023.145738)

[16] Y. Zhang, L. Tang, Y. Wang, J. Wang, J. Zhou, J. Lu, Y. Zhang, Z. Zhang, Development and application of a high-temperature imaging system for in-situ scanning electron microscope Materials Today Communications 38 (2024) 107782 (https://doi.org/10.1016/j.mtcomm.2023.107782)

[17] A. M. Brown, M. P. Hill, A hot stage SEM for gas-solid reaction studies. J. Microscopy (1989) 153[1] 51-62 (https://onlinelibrary.wiley.com/doi/pdf/10.1111/j.1365-2818.1989.tb01466.x)

[18] J. Mendonça, H.P. Brau, D. Nogues, A. Candeias, R. Podor, Development of a microfurnace dedicated to *in situ* SEM observation up to 1300°C - Part I: Concept, fabrication and validation. (Submitted)

[19] A. El Maakoul, B. Remy, A. Degiovanni, Modeling of thermal contacts with heat generation: Application to electrothermal problems. International Journal of Heat and Mass Transfer (2019) 140 293-302 (https://doi.org/10.1016/j.ijheatmasstransfer.2019.06.015)

[20] M.G. Cooper, B.B. Mikic, M.M. Yovanovich, Thermal contact conductance. International Journal of Heat and Mass Transfer (1969) Volume 12, Issue 3, Pages 279-300 (https://doi.org/10.1016/0017-9310(69)90011-8)

[21] C.V. Madhusudana, Thermal Contact Conductance, Second Edition, Mechanical Engineering Series, Springer International Publishing (2014) (https://doi.org/10.1007/978-3-319-01276-6)